Dynamics of Low-Intermediate–High-Confinement Transitions in Toroidal Plasmas

J. Cheng,[1] J. Q. Dong,[1,2,*] K. Itoh,[3] L. W. Yan,[1] M. Xu,[1] K. J. Zhao,[1,4] W. Y. Hong,[1] Z. H. Huang,[1] X. Q. Ji,[1]
W. L. Zhong,[1] D. L. Yu,[1] S.-I. Itoh,[5] L. Nie,[1,6] D. F. Kong,[6] T. Lan,[6] A. D. Liu,[6] X. L. Zou,[7]
Q. W. Yang,[1] X. T. Ding,[1] X. R. Duan,[1] Yong Liu,[1] and HL-2A Team

[1]*Southwestern Institute of Physics, Chengdu 610041, People's Republic of China*
[2]*Institute for Fusion Theory and Simulation, Zhejiang University, Hangzhou 310027, People's Republic of China*
[3]*National Institute for Fusion Science, Oroshi-cho, Toki 509-5292, Japan*
[4]*WCI Center for Fusion Theory, National Fusion Research Institute, Gwahangno 113, Yusung-gu, Daejeon 305-333, Korea*
[5]*Research Institute for Applied mechanics, Kyushu University, Kasuga, Kasuga koen 6-1, Fukuoka 816-8580, Japan*
[6]*Department of Modern Physics, USTC, Hefei 230026, People's Republic of China*
[7]*CEA, IRFM, F-13108 Saint-Paul-lez-Durance, France*

The dynamic features of the low-intermediate–high-(L-I-H) confinement transitions on HL-2A toka-mak are presented. Here we report the discovery of two types of limit cycles (dubbed type-Y and type-J), which show opposite temporal ordering between the radial electric field and turbulence intensity. In type-Y, which appears first after an L-I transition, the turbulence grows first, followed by the localized electric field. In contrast, the electric field leads type-J. The turbulence-induced zonal flow and pressure-gradient-induced drift play essential roles in the two types of limit cycles, respectively. The condition of transition between types-Y and -J is studied in terms of the normalized radial electric field. An I-H transition is demonstrated to occur only from type-J.

The existence of multiequilibrium states and transitions among them are common characteristics of complex systems with nonlinear interactions, and the related dynamics is an important field of nonlinear physics. In particular, identification of the key plasma parameters that control or determine the transition and reveal the physics mechanism of the low (L) to high (H) confinement transition in toroidal plasmas [1] has been a long-term focus of investigation and topic of interest. Understanding the transition physics is not only essential for assessing the power threshold scaling and ensuring heating requirements for future fusion reactors such as ITER [2] but also for involving development of nonlinear dynamics of complex systems. Meanwhile, the limit cycle oscillation (LCO) near the transition threshold has been studied theoretically, based on the bifurcation model [3] and the predator-prey model for zonal flow (ZF) and turbulence [4]. Study of the dynamical evolution of LCO in L-H transition with expansion of time scale provides opportunity to study the nonlinear mechanism quantitatively. In experiment, the dithering H-mode with characteristics of LCO was first observed on JFT-2M [5]. Such oscillations were also analyzed on AUG [6], JFT-2M [7], H-1 stellarator [8], TEXTOR with electrode biasing [9], and DIII-D [10] etc. Recently, it was observed on AUG that below the L-H threshold at low densities an LCO formed with competition between the turbulence level and the GAM flow [11]. On DIII-D, the evidence of predator-prey oscillations of a ZF with a frequency much below the GAM frequency preceding the L-H transition and periodic turbulence suppression were discussed when

the ZF shearing rate transiently exceeded the turbulence decorrelation rate [12]. A quasiperiodic oscillation of the radial electric field E_r at a frequency similar to the LCO predicted by the predator-prey model was observed preceding and following the L-H transition on EAST [13]. Similar oscillations were also observed propagating both radially inward or outward on TJ-II stellarator [14] and NSTX spherical tokamak [15]. Nevertheless, details of the dynamic features of the LCOs, including the causality and the condition for the onset, have not been identified. In particular, controversial results were also reported [16]. In this Letter, we report the discovery of two types of LCOs (dubbed type-Y and type-J, respectively), which show opposite temporal ordering to each other, on HL-2A toka-mak. The condition of transition between them is studied in terms of the normalized radial electric field. Type-Y appears first after an L-I transition, and the plasma comes back to L-mode if transition to type-J does not occur. An I-H transition is demonstrated to occur only from type-J. In the type-Y LCO, the turbulence intensity grows first, followed by localized flow, similar to preceding observations. In contrast, the type-J LCO is dominated by pressure-gradient-induced diamagnetic drift. The characteristics of the type-J LCO are presented in detail. Such a study on dynamical evolution provides opportunity to investigate the nonlinear mechanism quantitatively and is an essential step in understanding the physics of L-H transition quantitatively.

Experimental results from two shots of similar discharge parameters but different confinement features on HL-2A of

$R = 1.65$ m and $a = 0.40$ m are presented and compared for deuterium plasmas with lower single-null divertor configurations. The discharge parameters for the shot (labeled shot I) with L-I-H transitions are $B_t = 1.4$ T, $I_p = 180$ kA, $\bar{n}_e = (2.8-3.2) \times 10^{19}$ m^{-1}, $P_{NBI} = 1.0$ MW, while the parameters for the other (labeled shot II) with L-I-L transitions are $B_t = 1.4$ T, $I_p = 185$ kA, $\bar{n}_e = (2.5-3.0) \times 10^{19}$ m^{-1}, $P_{NBI} = 1.0$ MW. In fact, there are quite a few discharges that show the similar behavior of LCO for L-I-H and L-I-L transitions. The results presented in this Letter are well reproducible whenever the probe system is input into a plasma that has LCOs.

A four-step Langmuir probe array of 3×4 tips shown in Fig. 1 is used to measure the time evolutions of floating potential, electron density, and temperature in the edge region at the transitions. The diameter and the length of the probe are 2.5 and 3 mm, respectively, the poloidal separation and step height (the separation in the radial direction) are 5 and 3 mm, respectively. The local potential fluctuations, electron density and temperature, electron pressure gradient, radial electric field, $\mathbf{E} \times \mathbf{B}$ and its shear rate, etc. can be simultaneously estimated. Typically, the array is located at $\Delta r = -5 - -8$ mm, where Δr is the radial displacement from the separatrix, and the positive (negative) sign means outside (inside) the separatrix. In addition, the data acquisition frequency is $f_s = 1$ MHz with an accuracy of 12 bits.

Shown in Fig. 2 are time evolutions of the D_α signals [(a1) and (a2)], the spatio-temporal distributions of amplitudes of the floating potentials $|\phi_f|$ [(b1) and (b2)], radial electric field $|E_r| = |\nabla_r \phi_p| = |\nabla_r \phi_f + \alpha \nabla_r T_e|$ with $\alpha = 2.8$ [(c1) and (c2)], and the inverse scale lengths of electron pressure gradients $L_{pe}^{-1} = -\nabla_r p_e / p_e$ [(d1) and (d2)] in shots I and II, respectively. It is found that there are strong turbulent fluctuations of floating potentials and densities (not shown here) and weak radial electric fields in the L-modes. In contrast, the turbulent fluctuations of floating potentials and densities are weak, while the radial electric fields are rather strong in the I-phases. In addition, all the
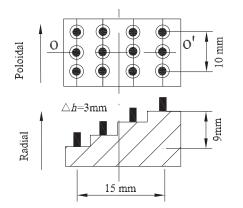
fluctuations oscillate at the same frequency of $f_{LCO} \simeq$ 2–3 kHz, which is identified to be close to the local ion-ion collision frequency. The modulations of floating potential and density are rather weak, while the radial electric field is very strong in the H-mode. All these observations are consistent with previous experimental results [5–15] and theoretical predictions [3,4]. It is worthwhile to point out that the density fluctuations and the radial electric fields do not correlate with each other in the L-modes but strongly correlate in the I-phases, exhibiting limit cycle oscillations (LCOs) [11–15], which are better illustrated in Fig. 3.

Given in Fig. 3 are the trajectories of the systems in the phase space of normalized radial electric field $X = e\rho_\theta |E_r| / \langle T_e \rangle$ (the abscissa axis) and the root mean square (rms) of the envelope of density fluctuations measured at $\Delta r = -5$ mm (the vertical axis) in shots I [(a)] and II [(b)], respectively. The trajectories are random in the L-modes but possess clear LCO features in the I-phases. The most important and interesting finding here is that the rotation direction reverses in shot I but does not in shot II. The first cycle (the open blue squares) for time $t = 505.5$–506 ms in shot I rotates in clockwise direction as predicted by the predator-prey model [4] and is dubbed type-Y LCO for convenience. However, the cycles for time $t = 510$–510.5 ms (the closed green triangles), $t = 518$–518.5 ms (the open black squares), and $t = 525$–525.5 ms (the open red squares) all rotate in counterclockwise direction, which is in contrast with the model and dubbed type-J LCO. On the other hand, the cycles for time $t = 536$–536.5 ms (the open blue squares), $t = 538.5$–539 ms (the closed green triangles), and $t = 543$–543.5 ms (the open brown squares) in shot II are all type-Y LCO. This is the central part of the discovery that is
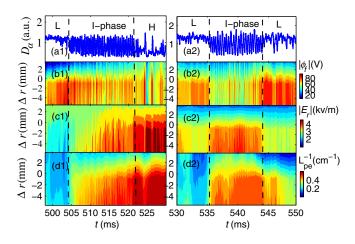

FIG. 1.   Sketch of the four-step probe array.

FIG. 2 (color online).   Time evolutions of D_α signals [(a1) and (a2)], the spatio-temporal distributions of the amplitudes of the floating potential $|\phi_f|$ [(b1) and (b2)] radial electric field $|E_r|$ [(c1) and (c2)], and the inverse scale lengths of electron pressure gradients L_{pe}^{-1}[(d1) and (d2)] for shots I and II.
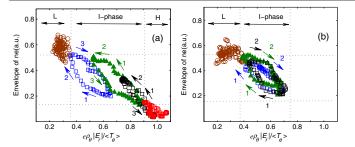
FIG. 3 (color online). Trajectories of the system in phase space of normalized radial electric field $|E_r|$ and rms of the density envelope (20–100 kHz) measured at $\Delta r = -5$ mm for shots I (a) and II (b).

FIG. 4 (color online). Bicoherence spectra estimated in 505–510 ms (a), 510–515 ms (b) and 515–520 ms (c), and the corresponding summed bicoherence spectra (d) in shot I.

reported in this Letter. There are, unambiguously, two types of LCOs, which show opposite temporal ordering to each other. In the type-Y LCO, the turbulence intensity grows first, followed by the increment of localized flow, similar to preceding observations in literature. In contrast, in the type-J LCO the radial electric field grows first, causing the reduction of fluctuations. The experimental data also indicate that in the I-phase, E_r at different radii change more or less in a similar way. Therefore, E_r shear and E_r change in a similar manner, and the conclusion does not change even if E_r shear instead of E_r is considered. By looking at the direction of the circulations and rejecting hypotheses that contradict basic physics principles, the plausible causality between the turbulence and radial electric field is figured out to be opposite in these two types of LCOs. In addition, type-Y appears first after an L-I transition, and the plasma comes back to L-mode if transition to type-J does not occur. An I-H transition is demonstrated to occur only from type-J. (It has to be pointed out that the data for the temperature and density of the ions are not available, and estimations such as $T_i \simeq 0.4 T_e$ and $Z_{\mathrm{eff}} \simeq 1$ may be made whenever they are required.)

The major difference between the experimental observations and the theoretical predator-prey model is that the plasma pressure and its gradient are taken as equilibrium parameters [4,17] without oscillation in the model but oscillate with LCO frequency in the experiments. On the other hand, contributions from zonal flow are not considered in the bifurcation model [3]. Actually, it is straightforward to see from the radial force balance equation of ions $E_r = (\nabla_r P_i)/(e n_i Z_{\mathrm{eff}}) + v_\phi B_\theta - v_\theta B_\phi$ that both flow (poloidal or toroidal) and pressure gradient may contribute to the balance of the radial electric field and, therefore, modulate turbulence and maintain LOCs. In the existing predator-prey model the roles of the zonal and mean flows in LCOs are emphasized, while the oscillation of pressure gradient is neglected. This may lead to the discrepancy between the model and the experimental observations of type-J LCOs. In order to verify such a speculation, a few aspects of the dynamics are examined as follows.
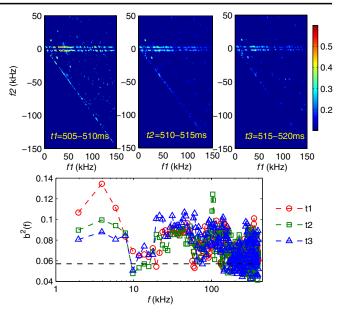
It is well accepted that ZFs are generated by turbulence via nonlinear three-wave interaction, which is manifested in bicoherence [18]. Shown in Fig. 4 are the bicoherence spectra (a-c) and the summed bicoherence spectra (d) of the turbulence in the periods of time in Fig. 3(a). The bicoherence is high in the zone of $f = f_1 + f_2 \simeq$ 2–3 kHz, where the summed bicoherence has a peak much higher than that at the rest in the first period of time. In contrast, the bicoherences and the summed bicoherences at $f \simeq$ 2–3 kHz are, respectively, low and comparable to the level at $f \simeq$ 20–100 kHz in the second and third periods. These results indicate that the LCO in the first period is dominated by ZF, while the LCOs in the second and third periods are not. In order to explore further in this direction the spatio-temporal distributions of amplitudes of the fluctuating floating potential $\delta\phi_f$, radial electric field $\delta\tilde{E}_r$, and electron density $\delta\tilde{n}_e$ of frequency $f \simeq$ 2–3 kHz are given in Fig. 5 for shots I (left column) and II (right column). It is clearly shown that $\delta\phi_f$ gradually decreases, while $\delta\tilde{E}_r$ and $\delta\tilde{n}_e$ increase in the I-phase prior to the I-H transition in shot I. In contrast, $\delta\phi_f$, $\delta\tilde{E}_r$, and $\delta\tilde{n}_e$ keep almost invariant in the whole I-phase in shot II. These observations indicate that it seems not likely that the turbulence-induced flows maintain the oscillation of the radial electric field and eventually induce I-H transition in the former. Then, a plausible candidate for maintaining the oscillation and eventually inducing I-H transition is the perturbation of the pressure gradient which must induce magnetic fluctuation of the same frequency due to the magnetohydrodynamic (MHD) equilibrium condition $\nabla P = \mathbf{j} \times \mathbf{B}$. In contrast, zonal flows are basically electrostatic perturbations with very low magnetic components
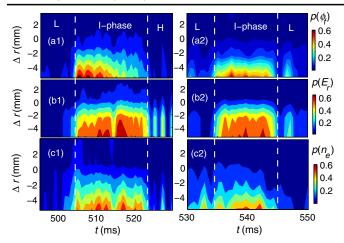
FIG. 5 (color online). Spatio-temporal distributions of amplitudes of fluctuating floating potential $\delta\phi$ (a1 and a2), radial electric field $\delta\tilde{E}_r$ (b1 and b2), and electron density $\delta\tilde{n}_e$ (c1 and c2) of frequency $f \simeq 2\text{–}3$ kHz for shots I and II.

[19]. Presented in Fig. 6 are (a) the time evolution of the spectrum of Mirnov coil signals $\partial B_\theta/\partial t$, (b) the coherence γ, and (c) phase shift spectra between $\partial B_\theta/\partial t$ and fluctuations of the gradient of electron pressure $\partial p_e/\partial r$, respectively, in the frequency range of 2–3 kHz. The intensity of the Mirnov coil signal is very weak in the L-mode and the first period of time of the I-phase. It increases gradually late and reaches a maximum prior to the I-H transition. In contrast, the intensity of the Mirnov coil signals (not shown here) is not noticeable during the whole discharge of shot II. The coherence reaches ~ 0.92 in the frequency range $f \simeq 2\text{–}3$ kHz and is much higher than that in the rest. In addition, the phase shift in the same frequency range is close to zero and in strong contrast to the rest. The poloidal and toroidal mode numbers of the magnetic fluctuations are identified as $m = 1$ and $n = 0$, respectively. The mode numbers of the Langmuir probe signals are not reliable owing to the too short poloidal and toroidal separations between the probes. It is worth pointing out that there are
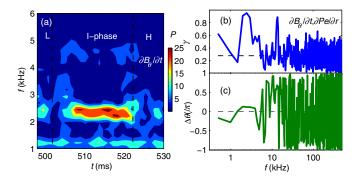

FIG. 6 (color online). Time evolutions of the spectrum of $\partial B_\theta/\partial t$ (a), the spectra of coherence γ (b) and phase shift (c) between $\partial B_\theta/\partial t$ and the gradient of electron pressure $\partial p_e/\partial r$ for shot I.

no sawtooth activities, and plasma confinement is improved in the later I-phase in shot I. Therefore, the possibility for MHD activity to cause the electric field oscillation could be eliminated.

There are two loops for the LCOs observed in the experiments. The first is the standard predator-prey model, where the turbulence increases first leading to generation of zonal flow which suppresses the former. Then the zonal flow decays due to lack of source and the turbulence grows again. The second is the bifurcation model, where the pressure gradient and corresponding radial electric field increase first, leading to decrease of turbulence. Then, the loop reaches a bifurcation point. The turbulence decreases further and the system enters H-mode if the pressure gradient and corresponding radial electric field are high enough to completely suppress the turbulence due to comparable driving and damping rates of the shear flow, or the turbulence increases again leading to decrease of the pressure gradient and eventually of the turbulence (lack of driving force), which leads to an increase of the pressure gradient and finishes the loop. From the experimental observations here it seems that the system must pass through an I-phase of type-J LCO to enter an H-mode under the discharge conditions described in this Letter. This discovery is a great step forward for understanding H-mode physics. This is because (i) the mechanism that induces H-mode transition should be the one that is dominant in the type-J LCOs, (ii) the condition of transition to type-J was also obtained in terms of the normalized radial electric field as $X \sim 1$ in Fig. 3(a).

In summary, two types of LCOs and transitions between them are found. The findings indicate that the two existing models for L-I-H transitions may describe two stages of a complete dynamic process, respectively. In this sense, the findings provide a unified dynamic picture of the transitions among L, type-Y LCO, type-J LCO, and H for the first time, which can resolve the previous controversial reports. Many more detailed theoretical and experimental investigations in this direction will certainly be stimulated to advance the understanding of H-mode physics significantly.

*Corresponding author.
jiaqi@swip.ac.cn

[1] F. Wagner *et al.*, Phys. Rev. Lett. **49,** 1408 (1982).

[2] T. Fukuda *et al.*, Nucl. Fusion **37,** 1199 (1997).

[3] S.-I. Itoh and K. Itoh, Phys. Rev. Lett. **60,** 2276 (1988).

[4] E. J. Kim and P. H. Diamond, Phys. Rev. Lett. **90,** 185006 (2003).

[5] S.-I. Itoh, K. Itoh, A. Fukuyama, and Y. Miura (JFT-2M Group), Phys. Rev. Lett. **67,** 2485 (1991).

[6] H. Zohm (ASDEX-UpgradeTeam/NI and ICRH Group), Phys. Rev. Lett. **72,** 222 (1994).

[7] T. Ido, Plasma Phys. Controlled Fusion **42,** A309 (2000).

[8] D. L. Rudakov, Plasma Phys. Controlled Fusion **43,** 559 (2001).

[9] S. Jachmich, G. Van Oost, R. R. Weynants, and J. A. Boedo, Plasma Phys. Controlled Fusion **40,** 1105 (1998).

[10] R. J. Colchin *et al.*, Phys. Rev. Lett. **88,** 255002 (2002).

[11] G. D. Conway, C. Angioni, F. Ryter, P. Sauter, and J. Vicente, Phys. Rev. Lett. **106,** 065001 (2011).

[12] L. Schmitz, L. Zeng, T. L. Rhodes, J. C. Hillesheim, E. J. Doyle, R. J. Groebner, W. A. Peebles, K. H. Burrell, and G. Wang, Phys. Rev. Lett. **108,** 155002 (2012).

[13] G. S. Xu *et al.*, Phys. Rev. Lett. **107,** 125001 (2011).

[14] T. Estrada, C. Hidalgo, T. Happel, and P. H. Diamond, Phys. Rev. Lett. **107,** 245004 (2011).

[15] S. J. Zweben, R. J. Maqueda, R. Hager, K. Hallatschek, S. M. Kaye, T. Munsat, F. M. Poli, A. L. Roquemore, Y. Sechrest, and D. P. Stotler, Phys. Plasmas **17,** 102502 (2010).

[16] G. R. Tynan *et al.*, IAEA FEC 2012 (San Diego), EX/10-3; G. R. Hill *et al.*, *ibid.*, OV/1-1.

[17] K. Miki, P. H. Diamond, Ö. D. Gurcan, G. R. Tynan, T. Estrada, L. Schmitz, and G. S. Xu, Phys. Plasmas **19,** 092306 (2012).

[18] Y. C. Kim, J. M. Beall, E. J. Powers, and R. W. Miksad, Phys. Fluids **23,** 258 (1980).

[19] L. Wang, J. Q. Dong, Y. Shen, and H. D. He, Phys. Plasmas **18,** 052506 (2011).